JOURNAL OF GEOPHYSICAL RESEARCH, VOL. 96, NO. E1, PAGES 15,599–15,616, AUGUST 25, 1991

Origin of Periodically Spaced Wrinkle Ridges on the Tharsis Plateau of Mars

THOMAS R. WATTERS

Center for Earth and Planetary Studies, National Air and Space Museum, Smithsonian Institution, Washington, D. C.

Ridged plains are a major geologic unit on Mars and are a predominant unit on the Tharsis Plateau, a region that has undergone uplift, extension, and extensive shield and flood volcanism. These units, probably flood volcanic in origin, are characterized by landforms classed as wrinkle ridges. Wrinkle ridges are interpreted to be folds, resulting from buckling followed by reverse to thrust faulting (flexure-fracture). A prominent characteristic of many of the wrinkle ridges on Mars, particularly those in the Tharsis ridge system, is the periodic nature of their spacing. The periodic spacing has been evaluated in six major provinces on the Tharsis Plateau with regions further divided into domains based largely on variation in ridge orientation. The average spacing of the Tharsis ridges, based on 2934 measurements, is 30 km. In an effort to account for the periodic nature of the wrinkle ridges, the ridged plains material is modeled as both a single member and a multilayer with frictionless contacts that has buckled at a critical wavelength of folding. Free slip between layers is assumed based on the possible existence of mechanically weak interbeds in the ridged plains sequence separating groups of flows. The near-surface mechanical structure in the area of ridged plains is approximated by a strong layer or layers overlying a weak megaregolith of finite thickness overlying a strong basement. Buckling of the ridged plains is assumed to be decoupled from the basement by the weak megaregolith. Decoupling is enhanced if the megaregolith were water- or ice-rich at the time of deformation. The rheologic behavior of the ridged plains and megaregolith is approximated by a linear elastic and linear viscous material. The models are examined for a range in (1) the strength contrast between the ridged plains material and the underlying megaregolith; (2) thickness of the ridged plains material; (3) thickness of the megaregolith; and (4) number of layers. The elastic model can explain the observed ridge spacing only if the ridged plains are relatively thick ($\geq$ 2400 m) with multiple layers ($n > 1$) and relatively high contrasts in Young's modulus ($E/E_0 \geq 100$). The high E/E_0 required is possible only if the megaregolith was water-rich at the time of deformation. Over the same range in values of the parameters, viscous buckling is much less restricted. The viscous model can explain the observed ridge spacing over a wide range in ridged plains thickness (250 m to several kilometers), megaregolith thickness, number of layers (n = 1 to 8) and contrasts in viscosity ($\eta/\eta_0 \geq 10$). In addition, viscous buckling is viable if the megaregolith were dry, water-rich or ice-rich at the time of deformation. The absence of folds with a cross-sectional geometry in the shape of a sinusoid (anticline-syncline pairs) may be the result of initial deformation of the ridged plains material into low-amplitude folds (in infinitesimal strain) followed by plastic yielding in the cores of the anticlines (in finite strain). Initial elastic or viscous buckling, coupled with plastic yielding confined to the hinge area followed by the development of reverse to thrust faulting, could account for the asymmetric fold geometry of many of the wrinkle ridges.

INTRODUCTION

Landforms referred to as mare or wrinkle ridges were first observed in mare basalts on the Moon. Analogous landforms have since been observed in smooth plains units on Mercury and Mars and in the lowlands of Venus. Wrinkle ridges are an assemblage of features consisting of long, narrow, relatively high relief ridges and broad, generally low-relief arches [*Watters*, 1988*a*]. Ridges can be subdivided into first-, second-, and third-order ridges on the basis of dimensions. First-order ridges, the largest in dimension, are generally asymmetric in cross section and often occur in en echelon arrangements. A variety of mechanisms have been proposed for the origin of the wrinkle ridges based solely on photogeologic investigations and limited field work on the Moon. They involve either intrusive or extrusive volcanism, tectonic deformation, or a combination of volcanism and tectonism.

In an analysis of a number of proposed analogs, *Plescia and Golombek* [1986] conclude that planetary wrinkle ridges are anticlines overlying reverse or thrust faults. The two kinematic models they suggest are (1) fault propagation folding in which a fold develops over an upward propagating reverse fault that eventually reaches the surface and (2) fault bend folding in which a fold results from a thrust sheet translated over a nonplanar surface. The anticlinal ridges in the Miocene flood basalts of the western Columbia Plateau are perhaps the best analogs for planetary wrinkle ridges [*Watters*, 1988*a*] and may provide the greatest insight into their origin. Thus wrinkle ridges are interpreted to be folds with reverse to thrust faulting developed as a result of buckling (flexure-fracture) rather than buckling a consequence of reverse or thrust faulting (fracture-flexure).

One of the largest known occurrences of wrinkle ridges on the terrestrial planets, observed within a distinct physiographic province, is on the Tharsis Plateau of Mars [*Watters and Maxwell*, 1986]. The tectonic setting of the Tharsis ridge system is, in many respects, different from the intercrater plains and basin provinces normally associated with the occurrence of wrinkle ridges on the Moon, Mercury, and other regions on Mars. An important characteristic of the ridges of the Tharsis Plateau is their apparent periodic spacing. This characteristic is common to ridges in other ridged plains provinces on Mars, as well as the anticlinal ridges of the Columbia Plateau [see *Watters*, 1989*a*].

The purpose of this investigation is to characterize the periodic spacing of the ridges of the Tharsis Plateau and to

Paper number 91JE01402

examine mechanisms for the origin of the spacing. The ridge system is divided into six provinces constituting contiguous units of ridged plains, and these provinces in some areas are further subdivided into domains based on variations in ridge orientation. Buckling models that may account for the periodic nature of the ridges are analyzed.

OBSERVATIONS

Tectonic Setting

The Tharsis region has been a major center of tectonic activity throughout the geologic history of Mars, experiencing uplift, extension, and extensive shield and flood volcanism. The topographic rise associated with the region encompasses over a quarter of the surface of the planet. One of the most extensive units on the plateau is the ridged plains material. The ridged plains units of Coprates, Lunae Planum, and Tempe Terra, on the eastern side of the Tharsis Plateau, alone have an areal extent of approximately 4×10^6 km^2 [*Scott and Tanaka*, 1986]. On the basis of indirect evidence such as the presence of volcanic landforms (i.e., flow fronts), the ridged plains material is interpreted to be flood volcanic in origin [*Scott and Tanaka*, 1986; *Greeley et al.*, 1977; *Basalt Volcanism Study Project* (BVSP), 1981; also see *Watters*, 1988*a*].

The morphology of the features in the Martian wrinkle ridge assemblages is virtually identical to their lunar analogs. The narrow, sinuous first-order ridges (Figure 1) are approximately 1–6 km wide and 100–600 m high [*Watters*, 1988*a*]. Many of the first-order ridges are capped or flanked by second-order ridges (width <1 km; height <200 m). Broad, gently sloping arches (average width about 9 km), similar to those in lunar mare, are associated with some of the Tharsis first-order ridges. A first-order ridge may coparallel or be superposed on an associated arch, as is often the case for mare ridges [*Strom*, 1972; *Maxwell et al.*, 1975].

The Tharsis Plateau ridge system is made up of hundreds of wrinkle ridges with orientations that are roughly circumferential to the regional topographic high and the major Tharsis volcanoes [*Watters and Maxwell*, 1986]. Many of the Tharsis ridges are crosscut by extensional fractures. Most of the fractures or graben have orientations radial to points near the center of the plateau [*Plescia and Saunders*, 1982]. Thus the intersection angle between the ridges and the crosscutting faults is often nearly orthogonal [*Watters and Maxwell*, 1983]. The Tharsis ridges appear to have formed roughly coincident with and, in some areas, prior to the formation of the crosscutting graben, in response to radially oriented compressive stresses.

In spite of the extensive tectonism observed on the Tharsis Plateau, Mars appears to be a one-plate planet [*Banerdt et al.*, 1982]. Models for the origin of the stresses in the Tharsis region are based on either lithospheric loading due to surface volcanics and/or shallow igneous intrusives [*Willemann and Turcotte*, 1982; *Solomon and Head*, 1982] or a combination of isostatically compensated uplift and loading [*Banerdt et al.*, 1982, 1991; *Sleep and Phillips*, 1985]. Analysis of these models relative to the Tharsis ridge system indicates that the location and orientation of stresses predicted by *Banerdt et al.* [1982, 1991] and *Sleep and Phillips* [1985] for isostatic adjustment best approximate the Tharsis ridge system [see *Watters and Maxwell*, 1986].

In addition to these large, contiguous areas on the Tharsis Plateau, there are many relatively small, isolated areas of ridged plains material that occupy topographic lows within intercrater plains [see *Scott and Tanaka*, 1986; *Greeley and Guest*, 1987]. Wrinkle ridges are also present in plains material that fill large impact basins on Mars. In Schiaparelli Basin, for example, the ridges are both basin concentric and periodically spaced [see *Mouginis-Mark et al.*, 1981]. In some of these areas the compressional stresses appear to be the result of local subsidence due either to loading from the ridged plains material or crustal cooling and volume reduction [see *Raitala*, 1987, 1988; *Watters and Chadwick*, 1989; *Wilhelms and Baldwin*, 1989].

Ridge Spacing

The periodic nature of ridge systems on Mars has been noted in a number of studies [*Saunders and Gregory*, 1980; *Saunders et al.*, 1981; *Watters and Maxwell*, 1985*a*, *b*]. The spacing of ridges in the Tharsis ridge system was analyzed in six major provinces of ridged plains material on the plateau. Some of the provinces were divided into domains on the basis of significant variation in orientation of the ridges and, in some areas, contacts with other geologic units. Provinces and their domains are shown in Figure 2. Using the 1:2,000,000 Controlled Photomosaics as a base, ridge spacing was determined using a series of sampling traverses spaced at roughly 12-km intervals oriented perpendicular to the predominant trend of the ridges in a given province or domain. The method used to determine ridge spacing includes all measurements between any two ridges along the sampling traverse. As a result, some of the measurements involve ridges that are not immediately adjacent. Also, since the frequency distribution of ridge spacing is strongly skewed or asymmetric (not Gaussian), the mode (the most frequently occurring observation) is a more reliable measure of the averaging spacing than the mean (Table 1 and Appendix A). The average spacing of the Tharsis ridges, excluding ridges on the intercrater plains of Memnonia, is 30 km (Figure 3).

As can be seen in Table 1, the average spacing within the domains of the Coprates province varies by as much as 30 km. Some of the variations in average spacing directly correlate with contacts of ridged plains material and Noachian highland terrain material or uplands. The ridge spacing and, in some cases, the relative amplitude of the ridges (relative to adjacent ridges imaged with the same viewing geometry) decrease rapidly as a contact between ridged plains and highland material is approached.

ANALYSIS AND MODELING

Previous and Recent Models

Saunders and Gregory [1980] and *Saunders et al.* [1981] were the first to investigate the periodic nature of the wrinkle ridges of the Tharsis Plateau and to suggest a deformational mechanism involving buckling at a dominant or critical wavelength. They employed a model proposed by *Biot* [1961] for viscous folding of a layered media. This model involves a viscous plate resting on a viscous half-space. The observed wavelengths can be accounted for with this model given a wavelength to thickness ratio of approximately 30

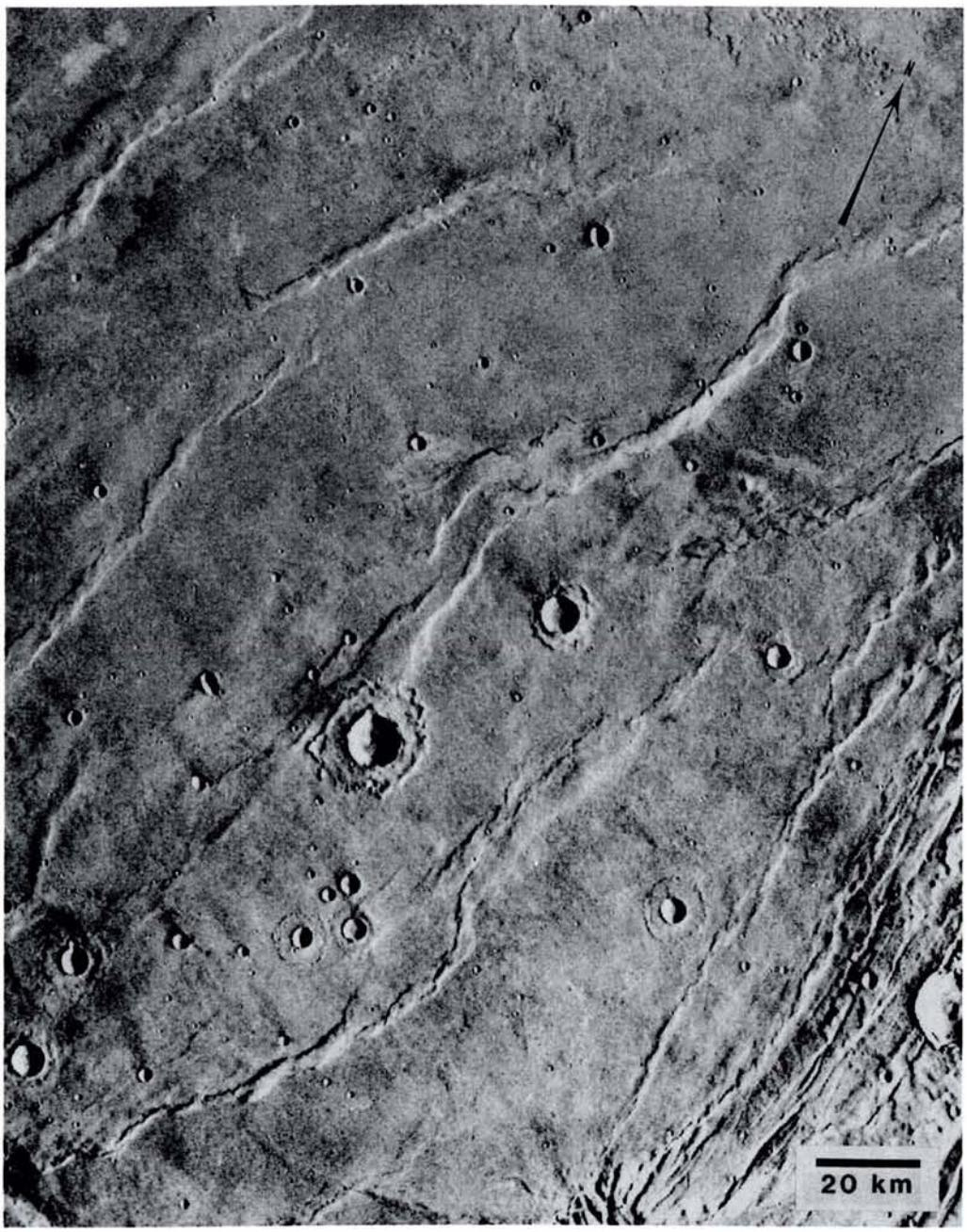

Fig. 1. Wrinkle ridges in the Coprates region of the Tharsis Plateau of Mars. These ridges are formed in ridged plains material and are morphologically and dimensionally similar to the anticlinal ridges of the Columbia Plateau. The ridges are narrow, sinuous, and strongly asymmetric in profile. Note contact between the ridged plains material and exposure of basement complex (bottom right of image) (Viking orbiter frame 608A26).

and a viscosity contrast between the ridged plains material and megaregolith substrate of approximately 500.

Watters and Maxwell [1985*b*] argue that the megaregolith can not be modeled as an infinite half-space and suggest that the fold geometry of the ridges could be influenced if the thickness of the megaregolith was small. Based on a study of the anticlinal ridges of the Columbia Plateau [*Watters*, 1989*a*], it has been argued that the ridged plains material should be modeled as a multilayer containing numerous thin interbeds and that the deformation is thin-skinned [*Watters*, 1988*b*, 1989*b*].

Zuber and Aist [1988, 1989] have examined a variety of compressional deformation models for the Martian lithosphere based on the Navier-Stokes equations for plane, quasi-static flow, evaluating linear and nonlinear viscosity and perfect plasticity. They model cases where the lithospheric basement is (1) free to deform (thick-skinned deformation) and (2) rigid (thin-skinned deformation). In their most recent study, *Zuber and Aist* [1990] model the ridged plains material as both a strong and weak surface layer. Models where the basement is involved in the deformation are preferred, and they suggest that ridge spacing may have been partially to completely controlled by the mechanical properties of the basement.

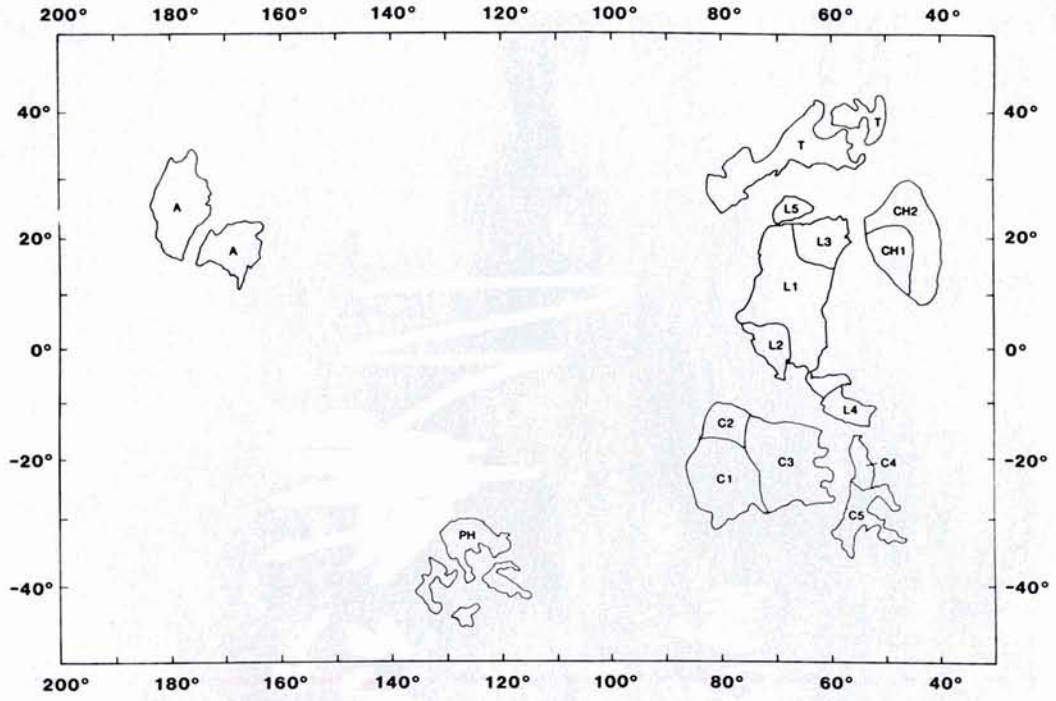

Fig. 2. Provinces and domains of the Tharsis ridge system. The spacing of ridges in the provinces of Coprates (C), Lunae Planum (L), Tempe Terra (T), Chryse Planitia (CH), Amazonis (A), and Phaethontis (PH) were determined using sampling traverses spaced at roughly 12 km intervals. Provinces were divided into domains on the basis of significant variations in ridge orientations (i.e., C1, C2, etc.). The average spacing for each of the provinces and domains is given in Table 1. The spacing of ridges that occur in the intercrater plains of Memnonia were not included because of their limited areal extent.

Near-Surface Physical and Mechanical Structure

The structure of the upper crust in the area of the ridged plains is assumed to consist of a mechanically strong sequence of volcanics analogous to mare basalts resting on a relatively weak megaregolith generated by intense bombardment of the bedrock. The underlying basement is presumed to be a mechanically strong, crystalline material perhaps analogous to the lunar highlands. Data on the near-surface structure of the Moon may provide useful constraints on modeling the mechanical structure on Mars. At the Apollo 17 landing site in the Taurus-Littrow valley, P wave velocities (V_p) of 960 and 4700 m/s are interpreted to be intact mare basalts overlying lunar highlands material [*Cooper et al.*, 1974]. Although the in situ measurements of V_p of the mare basalts are much lower than laboratory measurements, they are consistent with field measurements of terrestrial basalts [*Cooper et al.*, 1974, Figure 17]. Using these velocities and expected S wave velocities and densities, the approximate Young's modulus of the mare basalts and highland material are 2.5×10^9 and 5.8×10^{10} Pa, respectively. Thus based on this analogy, the contrast in Young's modulus between the

TABLE 1. Average Spacing of Ridges in the Tharsis Ridge System

Location	Mode, km	Mean, km	n
C1	50	72	269
C2	30	71	98
C3	50	57	435
C4	20	31	87
C5	20	45	64
L1	35	55	586
L2	30	47	107
L3	20	40	269
L4	30	78	104
L5	25	30	16
CH1	25	53	147
CH2	40	73	174
T	20	88	201
A	30	61	285
PH	20	43	92

Provinces and domains of the Tharsis ridge system: Coprates (C), Lunae Planum (L), Chryse Planitia (CH), Tempe Terra (T), Amazonis Planitia (A) and Phaethontis (PH). n is the number of measurements.

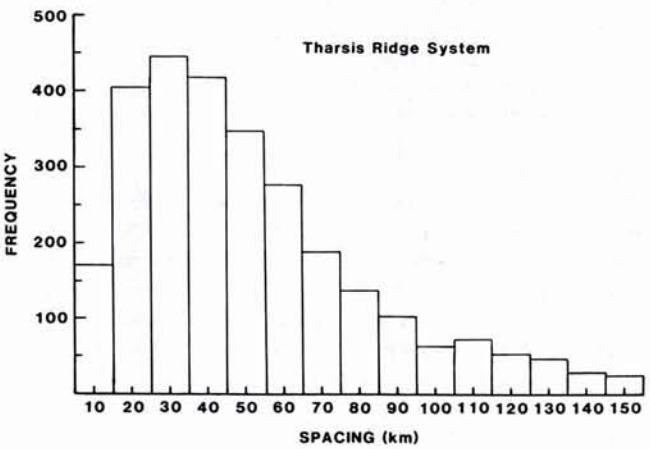

Fig. 3. Histogram of spacing of ridges in the Tharsis ridge system. The histogram includes all the spacing data from the provinces and domains shown in Figure 2.

ridged plains and basement would be expected to be on the order of 25. This is not a large strength contrast, but the effect is significant with the presence of a weak megaregolith. The strength and thickness of the megaregolith are discussed in the following sections. Since the estimated megaregolith thickness is much less than the observed wavelengths of the ridges, a shallow mechanical structure consisting of a strong layer(s) over a weak layer over a rigid basement is not an unreasonable approximation.

Thickness of the Ridged Plains

The thickness of the ridged plains material is poorly constrained. Using crater diameter and rim height relationships, estimates of greater than 0.25 km [*Frey et al.*, 1988], 0.5–1.5 km [*DeHon*, 1982], and 1.5 km [*Saunders and Gregory*, 1980] have been reported. However, there are a number of ambiguities inherent in this technique. In Coprates and Lunae Planum, the bulk of the craters used to estimate the thickness occur where ridged plains material encroaches on Noachian-aged highland terrain material. These estimates are then taken as an average thickness, based on the assumption that the elevation of the highland terrain underlying the ridged plains material is more or less constant. If the ridged plains are a multilayer consisting of a thick sequence of flows that occupy a topographic basin, the estimated thickness may be only that of the uppermost, margin-filling flows. The lack of certainty about the unit in which the partially buried crater was formed is a general problem with this method. The crater used in a given estimate may not be in highland terrain material but in a preexisting surface of the ridged plains material and the determined depth only a measure of the thickness of the upper-most flows. Thus these estimates may only represent a fraction of the total thickness of the ridged plains material.

An estimate of the apparent thickness of the ridged plains material can be obtained from exposures of the unit in the walls of Kasei Valles. *Robinson and Tanaka* [1988] identify two units in the Kasei Valles region based on their associated morphologic features. The upper unit is estimated to be on an average of 1000 m ± 200 m thick, consistent with shadow measurements made as part of this study. Erosion of the upper unit is characterized by the formation of either steep scarps or chaotic terrain. The depth to the top of the lower unit is uniform throughout the Kasei Valles region, within the errors of the measurements, from roughly longitude 65°W to 74°W (M. Robinson, personal communication, 1990). The lower unit is exposed on the floor of Sacra Fossae and forms a terrace approximately 50 km wide and 120 km long on the NW corner of Lunae Planum (Figure 4). A wrinkle ridge lies along the trend of a prominent first-order ridge and arch on the plateau and is interpreted to be part of that ridge. The existing topographic relief of the segment on the lower unit represents some fraction of the total structural relief (exposed by erosion) of the ridge on the plateau. Wrinkle ridges elsewhere on the lower unit are rare, and those landforms identifiable as ridges are heavily degraded [see *Robinson and Tanaka*, 1988].

Robinson and Tanaka [1988] observed layering in the lower unit in exposures in the channels (visible on the north rim of the channel shown in Figure 4) and conclude that it is composed of a sequence of lava flows with an estimated thickness of at least 2.5 km. Based on the apparent degradation of the upper unit in some areas into chaotic terrain, they conclude that (1) the upper unit is less competent than the lower unit; (2) the upper unit is capped by a thin layer of ridged plains material which is underlain by friable material (megaregolith); and (3) the lower unit is basement material. An interpretation that is equally consistent with the observations is that the upper and lower unit are both ridged plains material. The apparent weakness of the upper unit could be the result of a greater number of interbeds in this sequence of flows relative to the lower sequence. The presence of some wrinkle ridges in the lower unit suggests that the entire ridged plains section has deformed or buckled, consistent with the model proposed by *Watters* [1988*a*]. If this interpretation is correct, the total thickness of the ridged plains material in the Kasei Valles region may be in excess of 3.5 km. This is consistent with maximum thicknesses observed in the large terrestrial flood basalt provinces (Table 2). Thus estimates of the maximum thickness of the ridged plains material vary by greater than an order of magnitude.

Mechanical Nature of the Ridged Plains

Although the ridged plains material is interpreted to be a volcanic sequence, there is no direct evidence to refute alternative suggestions (i.e., sedimentary material). If, however, the ridged plains material do consist of a sequence of flows, it is possible that interbeds were either formed or deposited between pulses of flood volcanism. Evidence of layering has been recently discovered in units mapped as ridged plains exposed in Kasei Valles [*Chapman and Tanaka*, 1991], strongly suggesting that the ridged plains are a layered volcanic sequence.

Interbeds separating groups or units of flows are not uncommon within mare basalts on the Moon or in terrestrial continental flood basalt sequences. Subsurface radar reflectors have been detected by the Apollo 17 lunar sounder experiment (ALSE). Reflectors lie at depths of 0.9 and 1.6 km below the surface of Mare Serenitatis and at 1.4 km below the surface of Mare Crisium [*Peeples et al.*, 1978; *Maxwell and Phillips*, 1978]. They are interpreted to be the result of deep-lying density inversions consisting of a regolith or pyroclastic layer [*Peeples et al.*, 1978]. The thickness of the interbeds detected by ALSE is estimated to be on the order of several meters. Other interbeds, on the centimeter scale, could be present but would not have been detected by the instrument (T. Maxwell, personal communication, 1989).

Terrestrial continental flood basalt sequences commonly contain interbeds that may be composed of aeolian, fluvial or lacustrine sediments [*BVSP*, 1981]. Numerous sedimentary interbeds occur in the upper section of the basalt of the Columbia River flood basalt province. Evidence of thin interbeds has been found recently in well log data penetrating the oldest and thickest section of basalts (Grande Ronde Basalts) in the Yakima fold belt [*Reidel et al.*, 1989*a*]. These interbeds range in thickness form several centimeters to a meter. In addition, interbeds in the Grande Ronde are much less frequent north and south of the fold belt (S. Reidel, personal communication, 1988), indicating that the anticlines developed where the basalts overlie a thick sequence of mechanically weak sediments and where interbeds are present [see *Watters*, 1989*a*].

To date, there is no direct evidence of interbeds within the

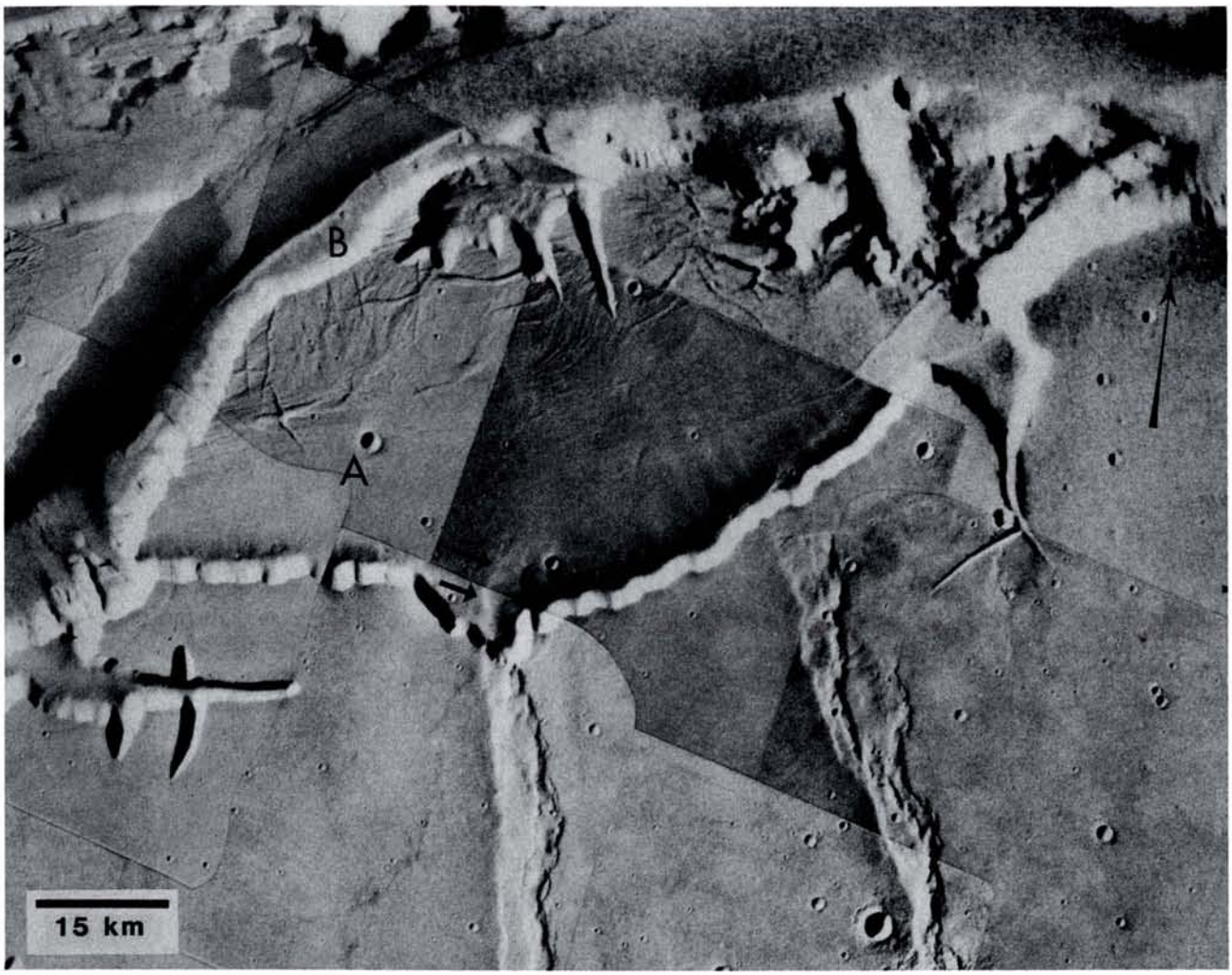

Fig. 4. Erosional terraces in the ridged plains material of northern Lunae Planum. The first terrace (A) lies approximately 900 m below the level of the ridged plains on the plateau. The second terrace (B) is roughly 1100 m below the level of the first. A segment of a ridge on the first terrace (arrow) lies along the trend of a prominent first-order ridge and arch on the plateau and is interpreted to be part of that ridge. The topographic relief of the segment on the terrace is interpreted to be a portion of total structural relief of the ridge on the plateau.

ridged plains material. However, if it is assumed that the mode of emplacement is analogous to that of the mare basalts and terrestrial continental flood basalts, the possible existence of interbeds cannot be ignored. In fact, given the evidence for aeolian process on Mars, it is not unreasonable to expect that thin interbeds composed of aeolian material were deposited between pulses of flood volcanism. Such is the case for the flood basalts of the Parana Basin in Paraguay and Brazil, where interbeds of aeolian sand are common [see *BVSP*, 1981].

TABLE 2. Properties of Some of the Largest Terrestrial Flood Basalt Provinces

Location	Maximum Thickness, km	Areal Extent, km^2
Siberia Platform*	3.5	1.5×10^6
Parana Basin*	1.5–1.8	1.2×10^6
Deccan Traps*	2.0	5.0×10^5
Columbia Plateau†	4.2	1.6×10^5
Karroo Province*	8.0–9.0	1.4×10^5
Lake Superior Basin*	8.0–12.0	1.0×10^5

BVSP [1989].
†*Reidel et al.* [1989*a*] and *Tolan et al.* [1989].

The presence of mechanically weak interbeds may have a dramatic influence on the overall mechanical strength of the ridged plains, particularly if they allow some degree of slip between groups of flows [see *Biot*, 1961; *Currie et al.*, 1961; *Johnson*, 1984; *Zuber and Aist*, 1990]. Different degrees of resistance to slip along layer contacts may also strongly influence the geometry of the folds [*Johnson and Pfaff*, 1989; *Pfaff and Johnson*, 1989].

Thickness of the Megaregolith

The ridged plains units on Tharsis are presumed to be underlain by an extensive, poorly consolidated megaregolith. The thickness of this megaregolith is also not well constrained. *Fanale* [1976] postulates that the upper limit of the thickness of the megaregolith is 2 km. *Carr* [1979] estimates a thickness of at least 10 km based on a comparison with the depth of seismic scattering observed on the

TABLE 3. Young's Modulus for a Variety of Different Soil Types

Material	E, Pa
Hard clay	6.895×10^6 to 1.724×10^7
Sandy clay	2.758×10^7 to 4.137×10^7
Silty sand	6.895×10^6 to 2.069×10^7
Loose sand	1.034×10^7 to 2.413×10^7
Dense sand	4.827×10^7 to 8.274×10^7
Dense sand and gravel	9.653×10^7 to 1.931×10^8

The values of Young's modulus E shown above are from *Kézdi and Mice* [1975].

Moon. *Woronow* [1988] estimates the cumulative impact flux on Mars to be three to five times the observed lunar highland density, which based on Monte Carlo simulation, corresponds to ejecta cover (i.e., megaregolith) that could be as thick as 5–10 km. His simulations indicate that the greatest distribution of ejecta thickness is at 5 km for the upper limit of the estimated cumulative flux. Thus an upper limit for the thickness of the megaregolith of 5 km is adopted.

Mechanical Nature of the Megaregolith

The mechanical properties of the megaregolith will vary greatly depending on whether volitales are present or the material is dry. Insight into the mechanical strength of a dry megaregolith on Mars may be obtained from seismic data on the lunar regolith. P wave velocities of lunar regolith are very low [*Watkins and Kovach*, 1973], averaging well over an order of magnitude below those in typical low-density rocks (i.e., volcanic breccia) [see *Christensen*, 1982]. The low velocities in the lunar regolith are attributed to brecciation and high porosity [*Watkins and Kovach*, 1973]. At the Apollo 17 landing site, the 100 m/s layer is interpreted to be lunar regolith and the 327 m/s layer is interpreted to be either older regolith, highly fractured bedrock or a mixture of the two [*Cooper et al.*, 1974]. The approximate Young's modulus of the two layers, using the in situ P wave and expected S wave velocities and densities, are 1.7×10^7 and 2.3×10^8 Pa, respectively. The Young's modulus of the regolith is within the range reported for terrestrial loose-sand soils (Table 3). The contrast in Young's modulus between mare basalt and the lunar regolith ranges from 10 to 150.

The mechanical strength or rigidity of a dry, unconsolidated, granular regolith will increase with depth as a result of compaction due to gravitational loading [see *Talwani et al.*, 1973]. If the megaregolith were dry at the time of ridge formation and is similar mechanically to lunar regolith, the difference in elastic modulus would be expected to be one order of magnitude, and in the most extreme case not in excess of two orders of magnitude. The effect of compaction can be reduced if the megaregolith was water-rich. *Carr* [1979] has suggested that confined aquifers several kilometers thick existed in the highly permeable megaregolith. Based on peak discharge rates necessary to generate large-scale channels, Carr estimates the pore pressure approached and potentially exceeded the lithostatic pressure. Perhaps the most dramatic examples of outflow channels occur on the eastern, western and northern margins of the ridged plains of Lunae Planum [*Carr*, 1979; *Scott and Tanaka*, 1986]. It is clear that the ridged plains of Lunae Planum were extensively eroded in the channel forming event. In addition to the hydrostatic head that would be expected due to the Tharsis rise [*Carr*, 1979, 1986], gravitational and tectonic loading will significantly contribute to the pore fluid pressure [*Hubbert and Rubey*, 1959]. Pore fluid pressure has been suggested as a mechanism to reduce frictional resistance to (1) slip between layers in a folding multilayer [*Biot*, 1961], and (2) movement of thrust sheets [*Hubbert and Rubey*, 1959; *Rubey and Hubbert*, 1959; *Hsu*, 1969*a*, *b*; *Forristall*, 1972]. If a high pore fluid pressure existed at the time of ridge formation, the strength contrast between the ridged plains material and the megaregolith, in terms of both Young's modulus and effective viscosity, may have been higher than two orders of magnitude. Another possibility is that a water-rich megaregolith is not chemically stable and the material would alter to clays resulting in an unindurated mud. Under these conditions, a contrast in Young's modulus of 100–1000 might be possible (see Table 3).

Alternatively, if the megaregolith were ice-rich at the time of ridge formation, under a tectonic stress its behavior can be approximated by a linearly viscous rheology with deformation resulting from viscous creep [*Squyres and Carr*, 1986; *Squyres*, 1989]. The apparent viscosity of rock glaciers may provide rough constraints on the viscosity of an ice-rich megaregolith. *Wahrhaftig and Cox* [1959] report apparent viscosities of up to 9.0×10^{13} Pa s for active rock glaciers. The viscosity of an ice-rich megaregolith would likely be at least several orders of magnitude higher due to perhaps a higher volume of granular material and confining pressure. However, the viscosity contrast between the megaregolith and the ridged plains material under these conditions, assuming the effective viscosity of the ridged plains material is on the order of the highest reported value for intact rock ($>2 \times 10^{21}$ Pa s) [*Handin*, 1966], would be high. The contrast in elastic strength, however, given these conditions would be expected to be low because the presence of ice in soils and rocks increases the P-wave velocity [see *Christensen*, 1982]. The association between valley networks, possibly formed by meltwater released from heating of ice-rich uplands, and the ridged plains material in the cratered uplands has been pointed out by *Wilhelms and Baldwin* [1989]. Thus it is possible that the ridged plains material associated with the Tharsis Plateau and on the rest of the planet overlies a once water or ice-rich megaregolith.

Model Assumptions

The models proposed in this study are based on beam theory. It is assumed that the ridged plains material has been deformed at the free surface in the brittle domain under little or no confining pressure and low temperatures. The rheologies chosen to approximate the behavior of the ridged plains material and megaregolith are a linear elastic and linear viscous material. It is important to consider elastic behavior because at low temperatures and pressures, ductility is rarely observed in rock [*Jaeger and Cook*, 1979, p. 228]. Viscous buckling models, however, do satisfactorily describe the wavelength to layer thickness ratio of terrestrial deformation at a variety of scales including the lithospheric scale [*Biot*, 1961; *Johnson*, 1984; *Zuber*, 1987].

Two end-member cases for the mechanical nature of the ridged plains material are examined, one in which the ridged plains behave as a single member and the other where the ridged plains behave as a series of plates with frictionless

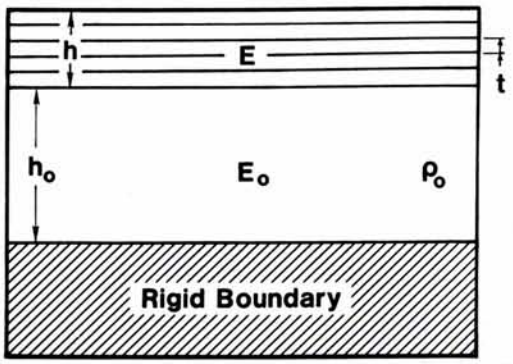

Fig. 5. Diagram of the boundary conditions. The ridged plains material are assumed to behave as either a single coherent layer or a multilayer with strength E resting on a mechanically weak substrate with strength E_0 and density ρ_0. In the case of a multilayer, frictionless contacts are assumed between the individual layers. The substrate is of finite thickness h_0 and is resting on a strong basement (rigid boundary) that does not participate in the deformation.

contacts. Although some resistance to slip is likely, the model can accommodate this condition by increasing the number of layers (n) for a given set of parameters. A range in both the thickness of the ridged plains material and the number of layers presumed to be present are evaluated. Resistance to slip at the interface of the ridged plains and the megaregolith is assumed to be zero (i.e., free slip). The ridged plains and megaregolith are assumed to rest on a strong basement or lithospheric half-space (Figure 5). Although the boundary between the basement and megaregolith is assumed to be discrete, it may be gradational as suggested in some exposures in Valles Marineris [*Lucchitta et al.*, 1991]. In this analysis, it is assumed that the basement does not directly participate in the deformation that results in the ridges; thus no assumption of whole or partial lithosphere deformation is necessary to explain the periodic spacing. This is not to suggest that tectonic stresses were not acting on the lithosphere at the time of ridged plains deformation. Stresses that penetrate the crust and lithosphere (basement) could result in thin-skinned deformation of the ridged plains that is decoupled from deformation of the lithosphere by a mechanically weak megaregolith. The likelihood of decoupling is enhanced if the megaregolith were water- or ice-rich at the time of deformation. The length scale of lithospheric deformation may be larger than that of the periodically spaced ridges, depending on the mechanical properties of the lithosphere [see *Watters*, 1987; *Zuber and Aist*, 1990].

Elastic Model

The deflection of an elastic plate, in infinitesimal strain, resting on a substrate at the free surface subjected to an in-plane horizontal end load is given by

$$D\frac{d^4w}{dx^4} + P\frac{d^2w}{dx^2} + kw = 0 \tag{1}$$

where w is the deflection and P is the horizontal force. The flexural rigidity D is related to the thickness of the elastic plate h by

$$D = \frac{Eh^3}{12(1-\nu^2)} \tag{2}$$

where E is Young's modulus and ν is Poisson's ratio [see *Turcotte and Schubert*, 1982; *McAdoo and Sandwell*, 1985]. In the case of a multilayer, $h = nt$, where n is the number of layers and t is the average thickness of a layer [*Biot*, 1961; *Currie et al.*, 1962]. The resistance of the substrate to bending is given by k in (1). The total resistance to bending consists of two components: (1) the elastic resistance of the substrate and (2) the hydrostatic restoring force or buoyancy which incorporates the influence of gravity (i.e., body forces). The restoring force which results from the replacement of substrate material in a vertical column by less dense material (in the case of deformation at the free surface, atmosphere) is given by

$$\rho_0 g \tag{3}$$

where ρ_0 is the density of the substrate and g is the acceleration due to gravity [see *Turcotte and Schubert*, 1982].

The thickness of the substrate is important in determining the elastic resistance to bending. *Johnson* [1984] has shown that in order for a medium of finite thickness to approximate one of infinite thickness, the ratio of thickness of the substrate to the wavelength of folding must be greater than 0.6 [also see *Currie et al.*, 1962]. Assuming the thickness of the megaregolith does not exceed 5 km, the substrate thickness to wavelength ratio for the ridges is of the order of 0.17 or less. The elastic resistance of a substrate of finite thickness can be approximated by assuming that the medium consists of a series of independent elastic columns, each with a Young's modulus of E_0 [*Currie et al.*, 1962; *Johnson*, 1984]. The force per unit length necessary to strain each column is given by E_0/h_0, where h_0 is the thickness of the substrate. Thus the total resistance to bending is given by

$$k = E_0/h_0 + \rho_0 g \tag{4}$$

The differential equation for the deflection of an elastic plate (1) has been solved for a number of relevant boundary conditions [*Hetenyi*, 1949; *Turcotte and Schubert*, 1982; *Johnson*, 1984]. It can be shown that a sinusoidal deflection of the plate in the form

$$w = C \sin(ax) \tag{5}$$

where C is a constant and a is the length scale, satisfies (1). When the end load reaches the elastic buckling limit P_c, the critical wavelength developed is given by

$$\lambda_c = 2\pi\left[\frac{Ent^3}{12(1-\nu^2)\rho_0 g}\left(\frac{1}{1+(E_0/\rho_0 g h_0)}\right)\right]^{1/4} \tag{6}$$

(Appendix B). From (6) it is clear that there is a direct relationship between the wavelength and the thickness of the ridged plains material, and that the wavelength is dependent on the Young's modulus of the ridged plains material and the underlying megaregolith, and buoyancy forces. Also, as E_0 or the ratio $E_0/\rho_0 g h_0$ approaches zero, (6) reduces to the solution for a elastic plate floating on a dense fluid [see *Turcotte and Schubert*, 1982].

The wavelength as a function of thickness has been determined for an n of 1, 2, and 3 over a range in contrast in

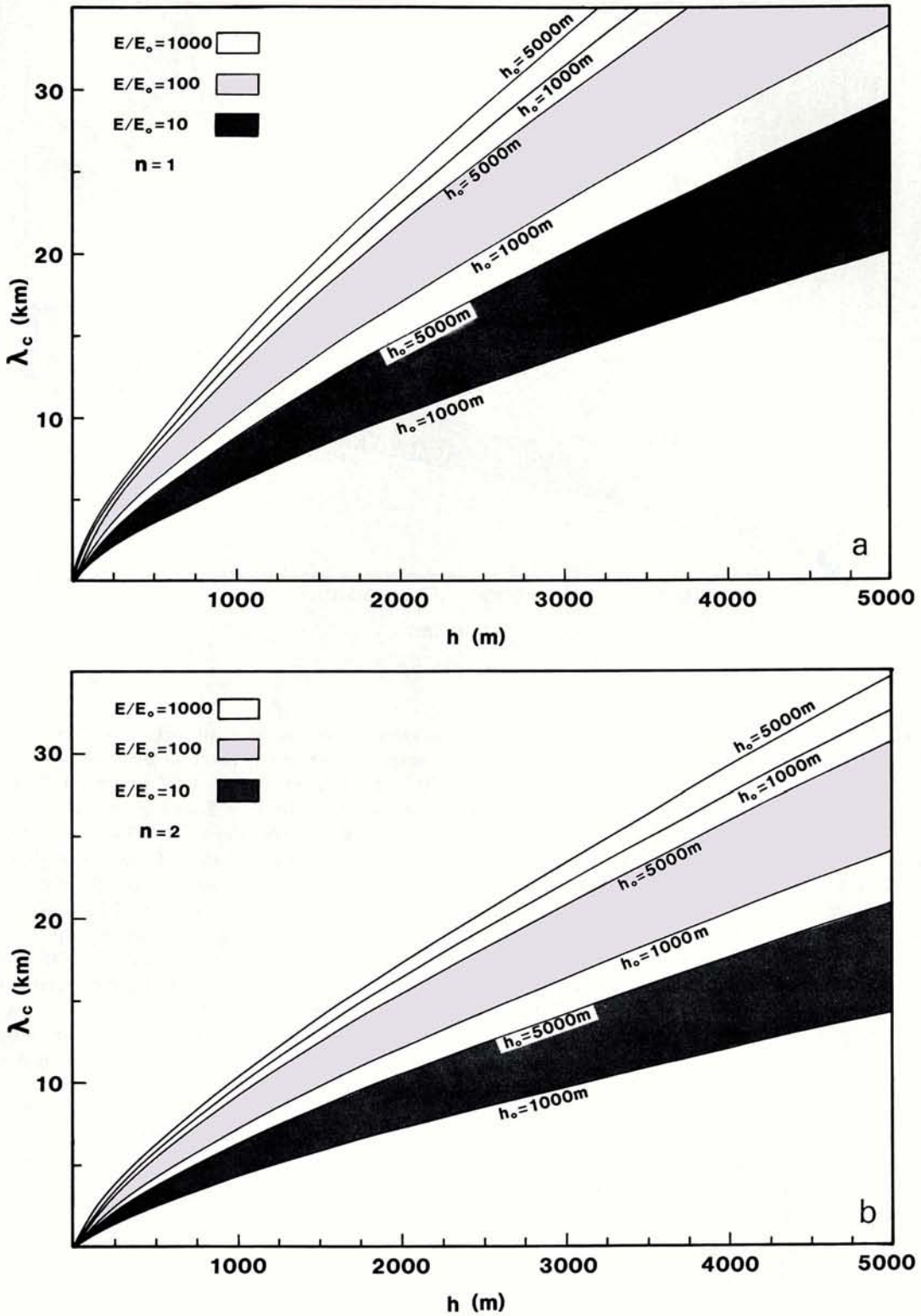

Fig. 6. The critical wavelength of buckling λ_c as a function of thickness of the ridged plains material h over a range in thickness of the substrate h_0 of 1000–5000 m, a ratio in Young's modulus between the surface layer(s) and substrate E/E_0 = 10 (dark shading), 100 (medium shading) and 1000 (light shading) for number of layers n of (*a*) 1, (*b*) 2, and (*c*) 3. The curves bounding the shaded areas are the solutions for the given model parameters. The shaded areas define a family of curves for solutions for h_0 between 1000 and 5000 m for the given parameters.

Young's modulus E/E_0 of 10, 100, and 1,000 and a range in thickness of the regolith substrate h_0 of 1 to 5 km (Figures 6*a*, 6*b*, and 6*c*). The range in contrast in Young's modulus is relative to the Young's modulus of basalt given in Table 4 and are not applicable to any E/E_0. The average density of Martian megaregolith, estimated at 1900 kg m^{-3}, is the maximum bulk density measured in a lunar regolith [*Carrier et al.*, 1973]. The values of the parameters used in the model

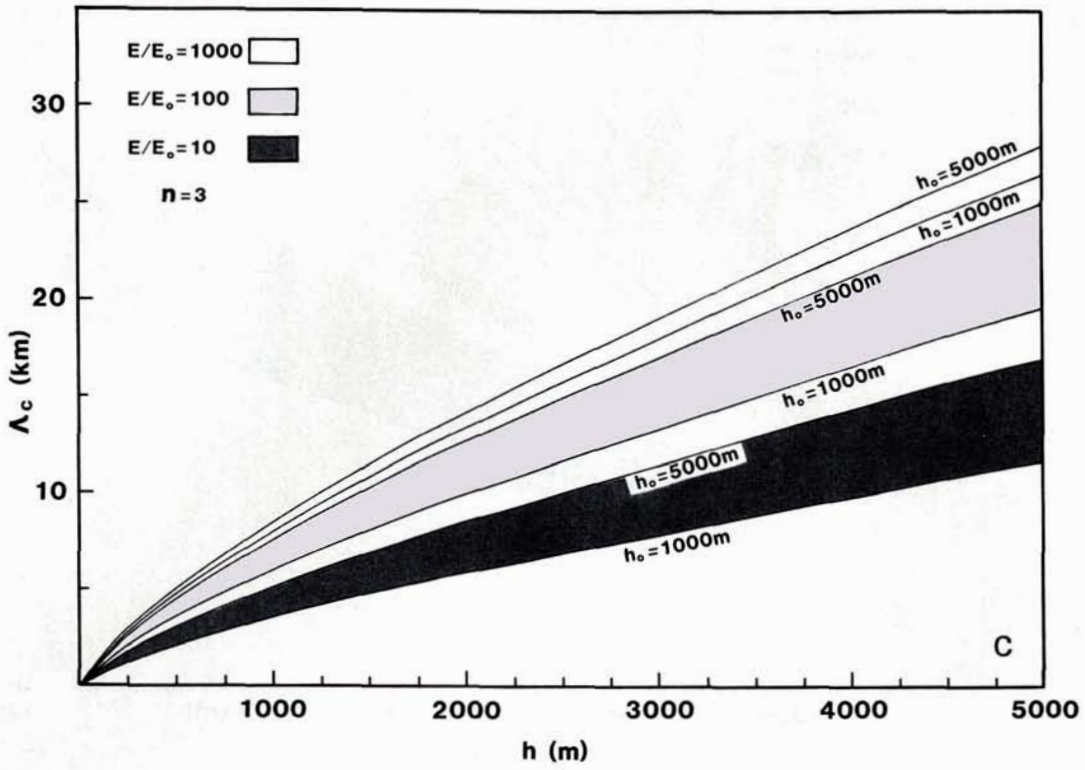

Fig. 6. (continued)

are given in Table 4. The case of $n = 1$ is equivalent to $h = t$, where the ridged plains sequence behave as a single layer with no interbeds (Figure 6*a*). Other cases of $n = 4$ and 5 were also examined. It is clear after inspection of Figure 6 that the wavelength decreases with an increase in n.

The strength of the material must be considered in determining the validity of a model based on elastic instability theory. In the upper crust, rock strength is controlled by the frictional resistance to brittle failure by sliding on randomly oriented fractures or joints [*Brace and Kohlstedt*, 1980; *Vink et al.*, 1984]. The frictional resistance and, thus, the maximum strength can be directly related to the normal and shear stresses by Byerlee's law:

$$\sigma_1 = 5\sigma_3, \qquad \sigma_3 < 110 \text{ MPa}$$
$$\sigma_1 = 3.1\sigma_3 + 210, \qquad \sigma_3 > 110 \text{ MPa} \tag{7}$$

expressed here in terms of the maximum (σ_1) and minimum (σ_3) principal effective stresses [after *Brace and Kohlstedt*, 1980]. The critical stress σ_c to achieve buckling is given by

$$\sigma_c = \left[\left(\frac{tEE_0}{3(1-\nu^2)h_0 n}\right) + \left(\frac{tE\rho_0 g}{3(1-\nu^2)n}\right)\right]^{1/2} \tag{8}$$

(Appendix B). For the case of $n = 1$ (Figure 6*a*), the critical stress exceeds the maximum compressive strength envelope of a rock with a mean density equal to that of terrestrial basalt ($\rho = 2900$ kg m^{-3}) over the entire range of E/E_0. At stresses above the maximum compressive strength, gross fracturing in the form of reverse or thrust faulting is favored over buckling. For $n > 1$, admissible wavelengths are obtained because with increasing n, the critical stress decreases. The critical stress as a function of thickness for the case of $n = 2$ (Figure 6*b*) is shown in Figure 7 along with the maximum compressive strength envelope. As indicated in Figure 7, there are no admissible wavelengths given $E/E_0 = 10$ for the range in thickness of the ridged plains considered.

Wavelengths for $n = 2$ case given $100 \geq E/E_0 \leq 1{,}000$ range from approximately 19 to 33 km for thicknesses of the ridged plains material ranging from 3800 to 4800 m and 1000 m $\geq h_0 \leq$ 5000 m. At the upper limit of the model parameters, for the case of $n = 2$, the minimum average spacing of the ridges (20 km) can be explained only if the ridged plains material is a minimum of 2400 m thick. For the case of $n = 3$, wavelengths range from approximately 9 to 27 km for thicknesses of the ridged plains of 1800 to 4800 m over the same range in the other model parameters. As discussed previously, a contrast in Young's modulus between the ridged plains and megaregolith of >10, and certainly >100, would require a water-rich megaregolith at the time elastic buckling occurred. Thus the elastic model is applicable, given the limits of the model parameters, only if the megaregolith was water-rich and the thickness of the ridged plains material was ≥ 2400 m at the time the observed wavelengths were established.

TABLE 4. Parameters for Model

Parameter	Definition	Value
E	Young's modulus (basalt)	2.5×10^9 Pa
η	Effective viscosity (basalt)	2.0×10^{21} Pa s
ρ_0	Megaregolith density	1900 kg m^{-3}
ν	Poisson's ratio (basalt)	0.25
g	Acceleration of gravity	3.75 m s^{-2}

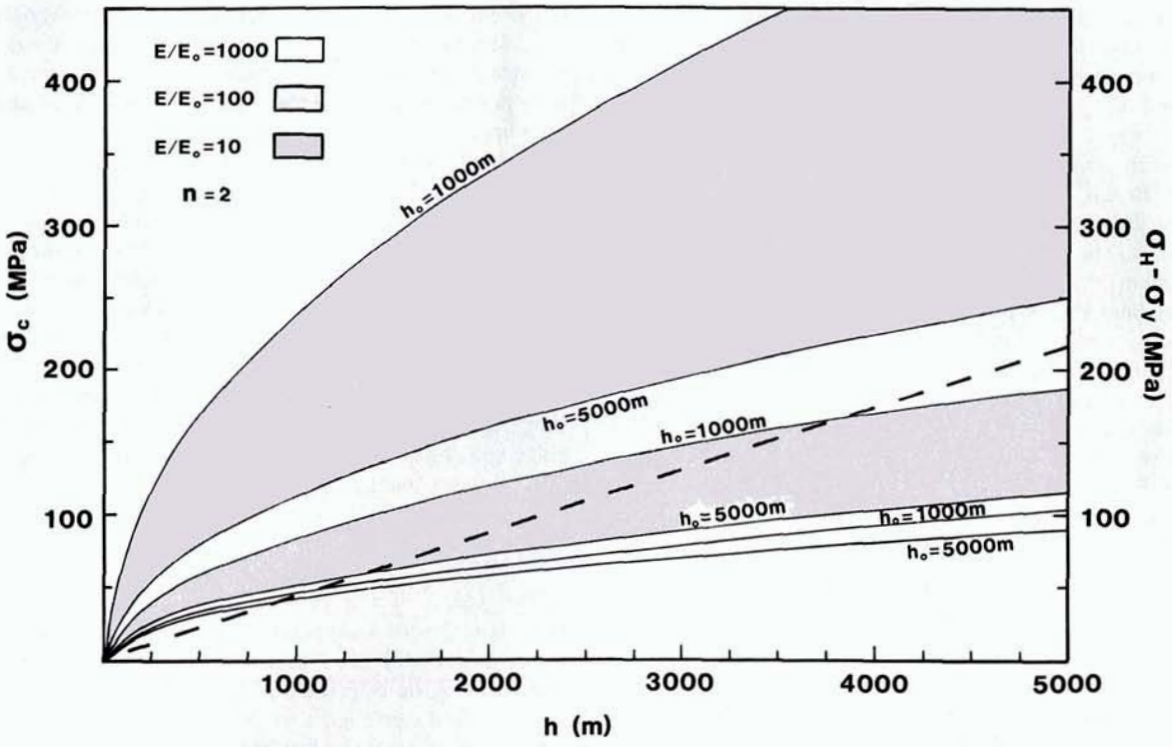

Fig. 7. The critical stress σ_c to achieve buckling as a function of thickness h for a range in thickness of the substrate h_0 of 1000–5000 m, a ratio in Young's modulus between the surface layers and substrate E/E_0 = 10, 100, and 1000 and n = 2 layers. The difference between the maximum horizontal and vertical stress is plotted as a function of depth. The dashed line represents the maximum compressive strength of a basalt-like material (ρ = 2900 kg m^{-3}) on the surface assuming no pore fluid pressure (dry rock). Critical stresses that fall above this line, in the shaded zone, exceed the maximum compressive strength of the material, and gross fracturing is expected over buckling.

Viscous Model

The linear viscous and linear elastic models are very similar because of the correspondence between the rheological equations [see *Johnson*, 1984]. The deflection of a viscous plate is given by

$$4\eta I \frac{\partial^5 w}{\partial x^4 \partial t} + P \frac{\partial^2 w}{\partial x^2} + \left(\frac{k}{n}\right) \frac{\partial w}{\partial t} + \frac{\rho_0 g w}{n = 0} \qquad (9)$$

where w is the deflection, η is the viscosity, and I is the moment of inertia. The resistance of the substrate to bending k is given by

$$k = \eta_0 / h_0 \qquad (10)$$

where E_0 in (4) has been replaced by the viscosity of the substrate η_0. In contrast to the elastic problem, buoyancy appear as an additional term in (9). For a multilayer, the resistance to bending acting on each layer is determined by dividing k and $\rho_0 g$ by the number of layers n [see *Biot*, 1961]. Equation (9) is satisfied by a sinusoidal deflection in the form of

$$w = g(t) \sin (ax) \qquad (11)$$

where $g(t)$ is some function of time. Substituting (11) into (9) and dividing through by sin $2\pi x/\lambda$ yields

$$b \frac{dg(t)}{dt} - g(t) = 0 \qquad (12)$$

where

$$b = \frac{4\eta_0 I(2\pi/\lambda)^2 + (k/n)(\lambda/2\pi)^2}{P[1 - (\rho_0 g/Pn)(\lambda/2\pi)^2]} \qquad (13)$$

The fastest growing wavelength for a given P will be that for which b is a minimum (see Appendix C). Minimization of b, however, does not result in a simple expression for the wavelength. It is clear from examination of (13) that as the denominator approaches zero, b approaches infinity. Thus, when the resistance to bending includes buoyancy, a critical load exists for viscous buckling. The wavelength that corresponds to this critical load is given by

$$\lambda = 2\pi \left[\frac{\sigma_c n t}{\rho_0 g}\right]^{1/2} \qquad (14)$$

This shows, as *Biot* [1959, 1961] demonstrated, that the influence of gravity makes the wavelength dependent on the load and has the effect of reducing the critical wavelength.

Dimensional analysis of the last two terms in (9) indicates that buoyancy can be neglected if the strain rate $\dot{e}$ is such that

$$\dot{e} \gg \rho_0 g h_0 / \eta_0 \qquad (15)$$

Over the range in viscosity and thickness of the megaregolith modeled, the strain rates range from 4×10^{-14} to 2×10^{-11} s^{-1}. The required strain rates would have to be at least greater by an order of magnitude. Although no estimates

exist, it can be argued that the strain rates involved in wrinkle ridge formation were rapid. This is based on the timing of deformation relative to the emplacement history of the flood volcanics. Evidence of flows ponded by lunar wrinkle ridges suggests that ridges formed contemporaneously with and following the emplacement of the mare basalts [*Bryan*, 1973]. Flows ponded by wrinkle ridges are common in mare basins and on the ridged plains of Mars. This is also the case on the Columbia Plateau. Evidence of embayment, thinning and pinch out of flows on the flanks of the anticlinal ridges have been documented [*Reidel*, 1984; *Anderson*, 1987; *Reidel et al.*, 1989*b*]. Flood basalt sequences like the Columbia River Basalt Group (CRBG) and the Deccan Basalt Group are typically emplaced in a relatively short period. For example, 87% of the volume of the CRBG was emplaced in roughly 1.4 m.y. [*Reidel et al.*, 1989*a*]. Strain rates must have been very rapid for sufficient structural relief to develop and embay flows. If the influence of buoyancy is minor, the critical wavelength is given by

$$\lambda_c = 2\pi\left[\frac{\eta n t^3 h_0}{3\eta_0}\right]^{1/4} \tag{16}$$

(see Appendix C).

The wavelength, as a function of thickness for a contrast in viscosity η/η_0 of 10, 100, 1000, and 5000, and the same range in thickness of megaregolith for $n = 1$, 4, and 8, is shown in Figures 8*a*, 8*b*, and 8*c*. As in the elastic case, the wavelength decreases with an increase in n. Viscous buckling can account for the observed wavelengths over a wide range of viscosity contrast, ridged plains thickness and substrate thickness for either a single layer or a multilayer. For the case of $n = 1$, the minimum average spacing of the ridges can be explained at the lower limit of η/η_0 (10) and h_0 (1000 m), if the ridged plains material is a minimum of 3100 m thick (see Figure 8*a*). At the upper limit of η/η_0 (5000) and h_0 (5000 m) for $n = 1$, the minimum average spacing of the ridges can be explained at the lower limit of the estimated thickness of the ridged plains material (250 m). As discussed previously, a viscosity contrast of as high as 5000 is probably not unreasonable and is well within the accepted range for competent geologic materials [see *Biot*, 1961]. Wavelengths for the case of $n = 4$ range from roughly 5 to 77 km for a thickness of the ridged plains material h ranging from 500 to 3500 m given 1000 m $\geq h_0 \leq$ 5000 m and $100 \geq \eta/\eta_0 \leq 5000$ (Figure 8*b*). In the case of $n = 8$, wavelengths range from 3 to 54 km for the same range in model parameters (Figure 8*c*). Viscous buckling is thus much less restricted than the elastic case and is viable if the megaregolith were dry, water-rich or ice-rich at the time of deformation.

Discussion

Influence of Megaregolith Thickness

Significant variations in the thickness of the megaregolith substrate will influence the buckling wavelength in both the elastic and viscous cases. In the elastic case, particularly for high contrasts in Young's modulus, a decrease in the thickness of the substrate results in a decrease in the critical wavelength (see Figures 6*a*, 6*b*, and 6*c*) and an increase in the critical stress (see Figure 7). An increase in strength contrast (E/E_0) has the effect of reducing the minimum thickness of the substrate necessary to accommodate buckling. This analysis also shows that for the elastic case, if the substrate thickness thins below a critical value, all other parameters remaining equal, fracturing will be favored over buckling.

In the viscous case, the effect of a decrease in the thickness of the substrate is the same observed in elastic buckling, a decrease in the critical wavelength (see Figures 8*a*, 8*b*, and 8*c*). An increase in the viscosity contrast (η/η_0) reduces the minimum thickness of the substrate necessary to induce a given wavelength. If the thickness of the megaregolith is small (<1000 m), viscous buckling at the observed wavelengths is possible given a large viscosity contrast (>5000). If the thickness and mechanical properties of the megaregolith substrate are roughly uniform, the variability in ridge spacing is likely due to variation in the thickness of the ridged plains material.

Fold Geometry

The shape of the deflection predicted by the buckling models is that of a sinusoid (i.e., anticlines and synclines of equal amplitude). The narrow anticlinal ridges and broad synclines of the ridged plains are not a good approximation to a sinusoid (see Figure 1). Many of the asymmetric ridges appear to have a narrow crestal hinge separating a long, straight, gently dipping limb [see *Watters*, 1988*a*], a characteristic shared by the analogous structures on the Columbia Plateau [see *Price*, 1982; *Anderson*, 1987]. This geometry is very similar to that of kink folds.

A large portion of the strain in the anticlinal ridges of the Columbia Plateau, excluding displacements on associated reverse to thrust faults [see *Watters*, 1988*a*], has been accomplished through cataclastic flow on layer-internal faults [*Price*, 1982]. The cataclastic behavior appears to occur in discrete locations within the folds where the stress exceeds the yield strength. This form of yielding may be approximated by plastic behavior. If the ridged plains material is a basalt-like rock that behaves like a plastic material in finite strain, the material would not be expected to bend very much before yielding [see *Johnson*, 1984]. With elastic or viscous buckling of the ridged plains material into low amplitude folds (within the domain of infinitesimal strain), plastic yielding may follow in the cores of the anticlines where compressive stresses are high [see *Currie et al.*, 1962], propagating in the direction of the free surface. Such behavior may serve to localize the amplification of the folds in the areas of the anticlines, resulting in folds with narrow crestal hinges and straight limbs. This mechanism would involve rapid closing of the folds and, with continued horizontal shortening, the development of reverse to thrust faulting [see *Watters*, 1988*a*]. This model is not inconsistent with the development of regularly spaced thrust faults [see *Currie et al.*, 1962] or kinematic models that suggest that certain morphology elements of wrinkle ridges may be fault controlled [*Plescia and Golombek*, 1986; *Golombek and Plescia*, 1989; *Golombek et al.*, 1989, 1991]. It is, however, necessary that buckling precede the development of the reverse or thrust faults. Thus elastic or viscous buckling, followed by localized plastic yielding and the eventual development of reverse to thrust faulting, may explain the periodic spacing and fold geometry of many of the ridges in the Tharsis ridge system.

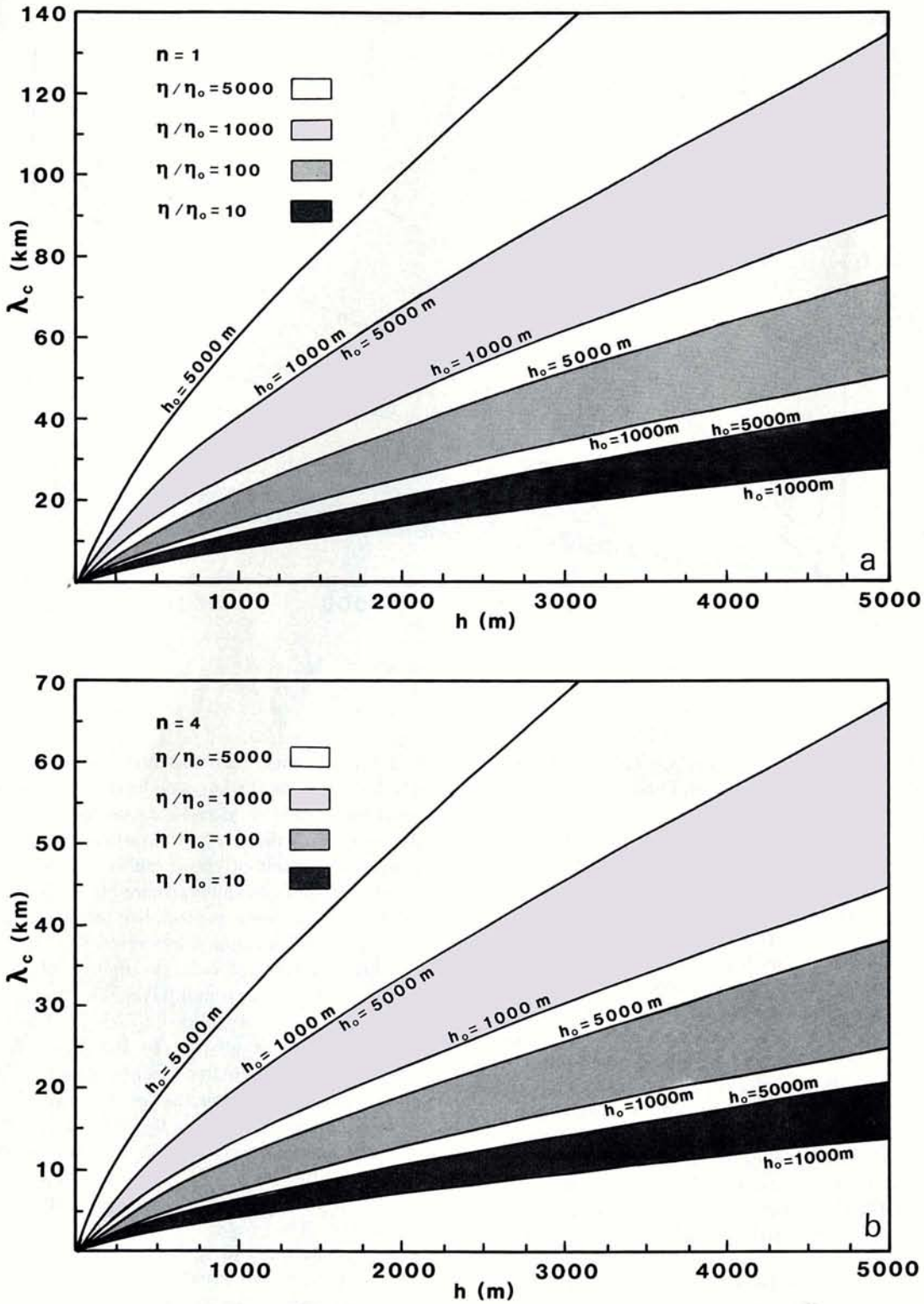

Fig. 8. The critical wavelength of buckling λ_c as a function of thickness of the ridged plains material h over a range in thickness of the substrate h_0 of 1000–5000 m, a ratio in viscosity between the surface layer(s) and substrate η/η_0 = 10 (darkest shading), 100 (dark shading), 1000 (medium shading) and 5000 (light shading) for number of layers n of (*a*) 1, (*b*) 4, and (*c*) 8.

SUMMARY

The ridged plains material of the Tharsis Plateau and other areas on Mars is probably flood volcanic in origin and are characterized by landforms classed as wrinkle ridges. The ridges are interpreted to be folds, resulting from buckling followed by reverse to thrust faulting (flexure-fracture). An important characteristic of many of the wrinkle ridges in the Tharsis ridge system is their periodic spacing. The average

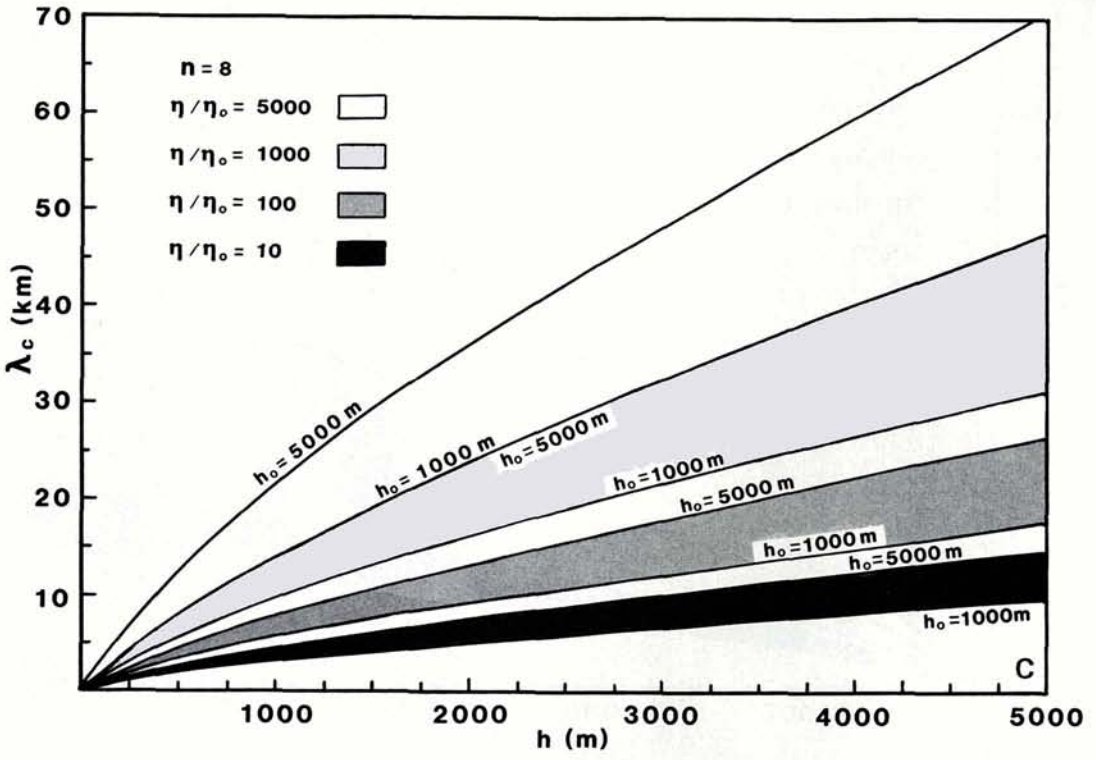

Fig. 8. (continued)

spacing, evaluated in six provinces (Coprates, Lunae Planum, Chryse, Tempe Terra, Amazonis, and Phaethontis) is 30 km (n = 2934).

The ridged plains material is modeled as both a single member and a multilayer with frictionless contacts. Free slip between layers is assumed based on the possible existence of mechanically weak interbeds consisting of either aeolian material or regolith in the ridged plains sequence separating groups of flows. Interbeds are common within terrestrial flood basalt sequences, and they have been detected in mare basalts in Mare Serenitatis and Mare Crisium on the Moon.

The near-surface mechanical structure in the area of ridged plains is approximated by a strong layer(s) overlying a weak megaregolith of finite thickness overlying a strong basement or lithosphere. Buckling of the ridged plains is assumed to be decoupled from the basement by a weak megaregolith of finite thickness. Decoupling is enhanced if the megaregolith were water- or ice-rich at the time of deformation. The rheologic behavior of the ridged plains and megaregolith are approximated by a linear elastic and linear viscous material.

An elastic and viscous buckling model is examined for a range in (1) the strength contrast between the ridged plains material and the underlying megaregolith; (2) thickness of the ridged plains material; (3) thickness of the megaregolith; and (4) number of layers n. For the elastic case, wavelengths consistent with many of the observed spacings are obtained at critical stresses below the yield-strength of a basalt-like material for $n > 1$. For $n = 2$, wavelengths range from 19 to 33 km for thicknesses of the ridged plains material ranging from 3800 to 4800 m given 1000 m $\geq h_0 \leq$ 5000 m and 100 $\geq E/E_0 \leq$ 1000. For $n = 3$, wavelengths range from 9 to 27 km over the same range in model parameters. The case of $n = 1$ (i.e., a single member) does yield admissible wavelengths. The average thickness of the ridged plains necessary to account for the minimum average spacing of the ridges, at the upper limit of h_0 and E/E_0, is roughly 2400 m. If the ridge spacing is the result of elastic buckling, the relatively high contrast in Young's modulus required ($\geq$ 100) is only possible if the megaregolith were water-rich at the time of deformation.

Viscous buckling is much less restricted and is applicable over a broader range of values of the model parameters for either a single layer or a multilayer. For the case of $n = 1$, the minimum average spacing of the ridges can be explained, at the upper limit of η/η_0 (5000) and h_0 (5000 m) and the lower limit of the estimated thickness of the ridged plains material (250 m). Wavelengths for the case of $n = 4$ range from roughly 5 to 77 km for a thickness of the ridged plains material h ranging from 500 to 3500 m given 1000 m $\geq h_0 \leq$ 5000 m and 100 $\geq \eta/\eta_0 \leq$ 5000. In the case of $n = 8$, wavelengths range from 3 to 54 km over the same range in model parameters.

The asymmetric fold geometry and broad, apparently undeformed inter-ridge areas that often characterize wrinkle ridges is inconsistent with the sinusoidal deflection (anticline-syncline pairs) predicted by the models. This may be explained by the initial deformation of the ridged plains material into low-amplitude folds (in infinitesimal strain) followed by plastic yielding in the cores of the anticlines (in finite strain) where stresses are highest. Plastic yielding confined to the hinge area would result in rapid closing of the fold and, with continued horizontal shortening, the eventual development of reverse to thrust faulting. This would account for the periodic spacing and the asymmetric fold geometry of the ridges.

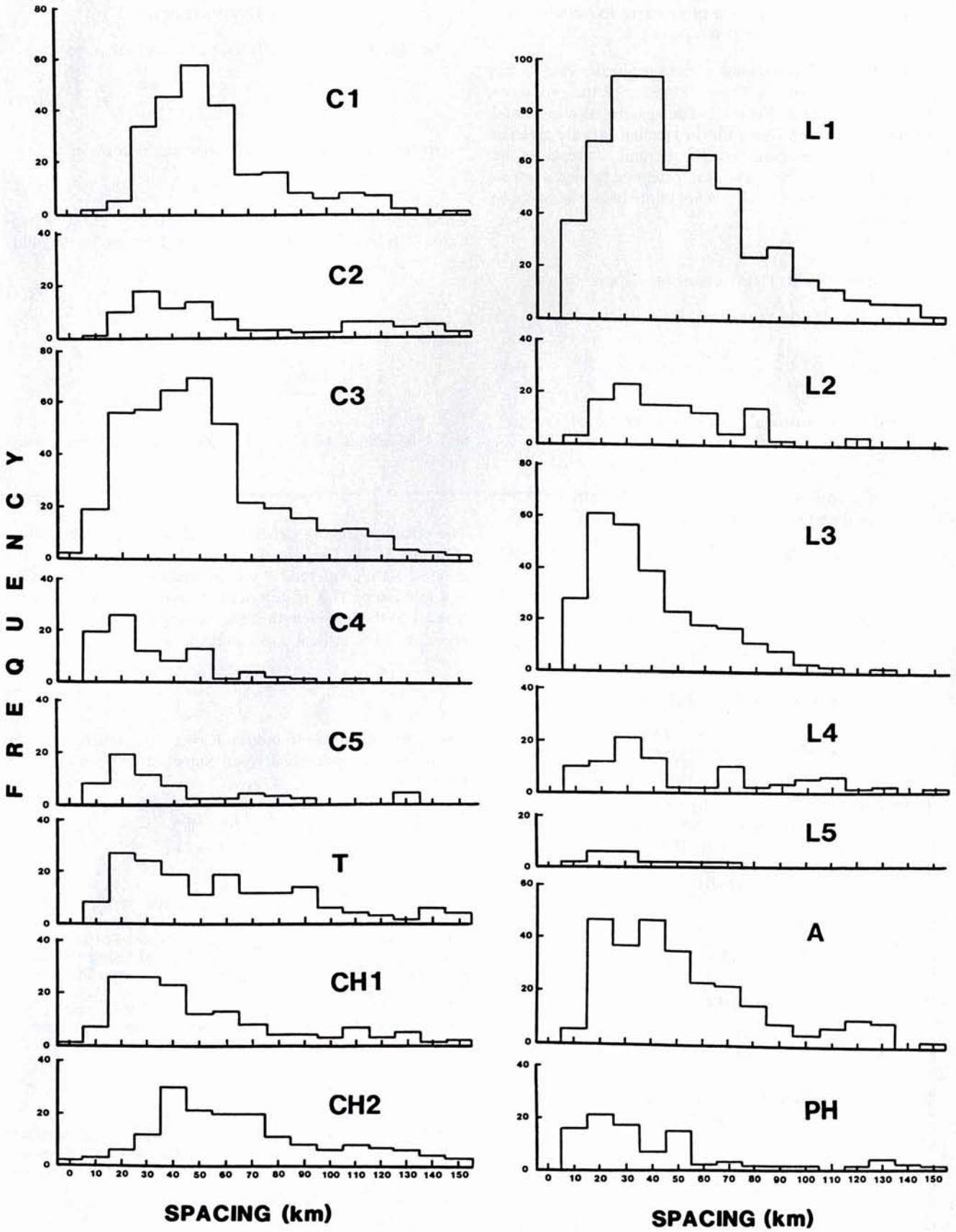

Fig. A1. Histograms of the spacing of ridges in the ridged plains units of the Tharsis Plateau for the provinces and domains shown in Figure 2.

APPENDIX A: RIDGE SPACING IN THE PROVINCES AND DOMAINS

Figure A1 shows histograms of the spacing of ridges in the ridged plains units of the Tharsis Plateau for the provinces and domains shown in Figure 2. The spacing data is binned in 10-km intervals. Statistics for the spacing data are given in Table 1. The skew evident in the histograms is a result of the sampling method. The spacings measured along a given sampling traverse include ridges not immediately adjacent to one another.

APPENDIX B: DERIVATION OF (6) AND (8)

The equation for the deflection of an elastic plate

$$D\frac{d^4w}{dx^4} + P\frac{d^2w}{dx^2} + kw = 0 \tag{B1}$$

is satisfied by a sinusoidal deflection given by (5)

$$w = C \sin (ax)$$

where C is a constant and $a = 2\pi/\lambda$. Substituting (5) into (B1) and dividing through by $C \sin 2\pi x/\lambda$ yields

$$Da^4 - Pa^2 + k = 0 \tag{B2}$$

where

$$a^2 = \frac{[P \pm (P^2 - 4Dk)^{1/2}]}{2D} \tag{B3}$$

Since $a = 2\pi/\lambda$, (A-3) can be written as

$$\left(\frac{2\pi}{\lambda}\right)^2 = \frac{[P \pm (P^2 - 4Dk)^{1/2}]}{2D} \tag{B4}$$

In order for the wavelength λ to be real, the applied load must reach a critical value P_c defined by setting the term under the radical in (B4) to zero. Thus

$$P_c = (4Dk)^{1/2} \tag{B5}$$

Then (B4) reduces to

$$(2\pi/\lambda)^2 = P/2D \tag{B6}$$

Substituting P_c for P in (B6) the critical wavelength is given by

$$\lambda_c = 2\pi(D/k)^{1/4} \tag{B7}$$

Substituting (2) where $h = nt$ and equation (4) into (B7) yields

$$\lambda_c = 2\pi\left[\frac{Ent^3}{12(1-\nu^2)\rho_0 g}\left(\frac{1}{1 + (E_0/\rho_0 g h_0)}\right)\right]^{1/4}$$

The expression for the critical stress is obtained by substituting (2) and (4) into (B6) and replacing P_c with $\sigma_c nt$ yielding

$$\sigma_c = \left[\left(\frac{tEE_0}{3(1-\nu^2)h_0 n}\right) + \left(\frac{tE\rho_0 g}{3(1-\nu^2)n}\right)\right]^{1/2}$$

APPENDIX C: DERIVATION OF (12)

The equation for the deflection of a viscous plate

$$4\eta I\frac{\partial^5 w}{\partial^4 x \partial t} + P\frac{\partial^2 w}{\partial x^2} + \left(\frac{k}{n}\right)\frac{\partial w}{\partial t} = 0 \tag{C1}$$

is satisfied by a sinusoidal deflection in the form of

$$w = g(t) \sin (ax) \tag{C2}$$

where $g(t)$ is some function of time and $a = 2\pi/\lambda$. Substituting (C2) into (C1) and dividing through by $\sin 2\pi x/\lambda$ yields

$$b\frac{dg(t)}{dt} - g(t) = 0 \tag{C3}$$

where

$$b = \frac{4\eta I(2\pi/\lambda)^2 + (k/n)(\lambda/2\pi)^2}{P} \tag{C4}$$

and k is defined by (10). Rearranging (C3) and integrating yields

$$g(t) = C \exp (t/b) \tag{C5}$$

The equation for the deflection is obtained by substituting (C5) into (C2). The wavelength that will be amplified the greatest for a given load P will be that for which b, in (C4), is a minimum. This is determined by differentiating b with respect to the wavelength λ and setting the results equal to zero. Thus the critical wavelength is given by

$$\lambda_c = 2\pi\left[\frac{4\eta n I h_0}{\eta_0}\right]^{1/4} \tag{B6}$$

where the moment of inertia $I = t^3/12$, where t is the thickness of an individual layer. Substituting the expression for I yields

$$\lambda_c = 2\pi\left[\frac{\eta n t^3 h_0}{3\eta_0}\right]^{1/4}$$

Acknowledgments. I am indebted to Bill McKinnon for his thorough reviews and insights into the models. I thank Maria Zuber and the anonymous reviewers for their reviews, Ted Maxwell for many useful discussions on wrinkle ridges, and Sean Solomon and Jeff Goldstein for helpful discussions on the modeling. I thank Michael Tuttle and John Chadwick for their assistance in data collection and in preparing the figures. I also thank Donna Slattery for typing and Priscilla Strain and Nancy Watters for editing the manuscript. This research was supported by NASA grant NAGW-940 and NAGW-1106.

REFERENCES

Anderson, J. L., The structural geology and ages of deformation of a portion of the southwest Columbia Plateau, Washington and Oregon, Ph.D. dissertation, 283 pp., Univ. of South. Calif., Los Angeles, 1987.

Basaltic Volcanism Study Project, *Basaltic Volcanism on the Terrestrial Planets*, 1286 pp., Pergamon, New York, 1981.

Banerdt, W. B., R. J. Phillips, N. H. Sleep, and R. S. Saunders, Thick shell tectonics on one-plate planets: Applications to Mars, *J. Geophys. Res.*, *87*, 9723–9733, 1982.

Banerdt, W. B., M. P. Golombek, and K. L. Tanaka, Stress and tectonics on Mars, *Mars*, edited by H. H. Kieffer et al., University of Arizona Press, Tucson, in press, 1991.

Biot, M. A., The influence of gravity on the folding of a layered viscoelastic medium under compression, *J. Franklin Inst. 267*, 211–228, 1959.

Biot, M. A., Theory of folding of stratified viscoelastic media and implications in tectonics and orogenesis, *Geol. Soc. Am. Bull., 72*, 1595–1620, 1961.

Brace, W. F., and D. L. Kohlstedt, Limits on lithospheric stress imposed by laboratory experiments, *J. Geophys. Res., 85*, 6248–6252, 1980.

Bryan, W. B., Wrinkle-ridges as deformed surface crust on ponded mare lava, *Proc. Lunar Sci. Conf., 4th*, 93–106, 1973.

Carr, M. H., Formation of Martian flood features by release of water from confined aquifers, *J. Geophys. Res., 84*, 2995–3007, 1979.

Carr, M. H., Mars: A water-rich planet, *Icarus, 68*, 187–216, 1986.

Carrier, W. D., J. K. Mitchell, and A. Mahmood, The relative density of lunar soil, *Proc. Lunar Sci. Conf., 4th*, 2403–2411, 1973.

Chapman, M. G., and K. L. Tanaka, Channeling episodes of Kasei Valles, Mars, and the nature of the ridged plains material (abstract), *Lunar Planet. Sci. XXII*, 197–198, 1991.

Christensen, N. I., Seismic velocities, in *Handbook of Physical Properties of Rocks*, edited by R. S. Carmichael, pp. 1–228, CRC Press, Boca Raton, Fla., 1982.

Cooper, M. R., R. L. Kovach, and J. S. Watkins, Lunar near-surface structure, *Rev. Geophys., 12*, 291–308, 1974.

Currie, J. B., H. W. Patnode, and R. P. Trump, Development of folds in sedimentary strata, *Geol. Soc. Am. Bull., 73*, 655–674, 1962.

DeHon, R. A., Martian volcanic materials: Preliminary thickness estimates in the eastern Tharsis region, *J. Geophys. Res., 87*, 9821–9828, 1982.

Fanale, F. P. Martian volatiles: Their degassing history and geochemical fate, *Icarus, 28*, 179–202, 1976.

Forristall, G. Z., Stress distributions and overthrust faulting, *Geol. Soc. Am. Bull., 83*, 3073–3082, 1972.

Frey, H., J. Semeniuk, and T. Grant, Early resurfacing events on Mars (abstract), in *MEVTV Workshop: Early Tectonic and Volcanic Evolution of Mars*, pp. 24–26, Lunar and Planetary Institute, Houston, Tex., 1988.

Golombek, M. P., and J. B. Plescia, Subsurface structure of martian wrinkle ridges (abstract), in *Fourth International Conference on Mars, Programs and Abstracts*, pp. 113–114, NASA, Tucson, Ariz., 1989.

Golombek, M. P., J. Suppe, W. Narr, J. Plescia, and B. Banerdt, Involvement of the lithosphere in the formation of wrinkle ridges on Mars (abstract), in MEVTV Workshop on Tectonic Features on Mars, edited by T. R. Watters and M. P. Golombek, *LPI Tech. Rep. 89-06*, pp. 36–38, Lunar and Planet. Inst., Houston, Tex., 1989.

Golombek, M. P., J. B. Plescia, and B. J. Franklin, Faulting and folding in the formation of planetary wrinkle ridges, *Lunar Planet Sci., XXI*, 679–693, 1991.

Greeley, R., and J. E. Guest, Geologic map of the eastern equatorial region of Mars, *Map I-1802-B*, U.S. Geol. Surv., Denver, Colo., 1987.

Greeley, R., and P. D. Spudis, Volcanism on Mars, *Rev. Geophys., 9*, 13–41, 1981.

Greeley, R., E. Theilig, J. E. Guest, M. H. Carr, H. Masursky, and J. A. Cutts, Geology of Chryse Planitia, *J. Geophys. Res., 82*, 4039–4109, 1977.

Handin, J., Strength and ductility, in Handbook of Physical Constants, edited by S. P. Clark, Jr., *Mem. Geol. Soc. Am., 97*, 223–300, 1966.

Hetenyi, M., *Beams on Elastic Foundation*, 255 pp., University of Michigan Press, Ann Arbor, 1949.

Hsu, K. J., A preliminary analysis of the statics and kinetics of the Glarus overthrust, *Eclogae Geol. Helv., 62*, 143–154, 1969*a*.

Hsu, K. J., Role of cohesive strength in the mechanics of overthrust faulting and of landsliding, *Geol. Soc. Am. Bull., 80*, 927–952, 1969*b*.

Hubbert, M. K., and W. W. Rubey, The role of fluid pressure in mechanics of overthrust faulting, *Geol. Soc. Am. Bull., 70*, 201–252, 1959.

Jaeger, J. C., and N. G. W. Cook, *Fundamentals of Rock Mechanics*, 3rd ed., 593 pp., Chapman and Hall, London, 1979.

Johnson, A. M., *Physical Processes in Geology*, 2nd ed., 577 pp., Freeman and Cooper, San Francisco, Calif., 1984.

Johnson, A. M., and V. J. Pfaff, Folding in layered media (abstract), in MEVTV Workshop on Tectonic Features on Mars, edited by T. R. Watters and M. P. Golombek, *LPI Tech. Rep. 89-06*, pp. 39–40, Lunar and Planet. Inst., Houston, Tex., 1989.

Kézdi, A., and C. E. Mice, Pile foundations, in *Foundation Engineering Handbook*, edited by H. F. Winterkorn and H. Fang, pp. 556–600, Van Nostrand Reinhold, New York, 1975.

Lucchitta, B. K., G. D. Clow, P. E. Geissler, A. S. McEwen, R. B. Singer, S. W. Squyres, and R. A. Schultz, The canyon systems on Mars, in *Mars*, edited by H. H. Kieffer et al., University of Arizona Press, Tucson, in press, 1991.

Maxwell, T. A., and R. J. Phillips, Stratigraphic correlation of the radar-detected subsurface interface in Mare Crisium, *Geophys. Res. Lett., 5*, 811–814, 1978.

Maxwell, T. A., F. El-Baz, and S. W. Ward, Distribution, morphology, and origin of ridges and arches in Mare Serenitatis, *Geol. Soc. Am. Bull., 86*, 1273–1278, 1975.

McAdoo, D. C., and D. T. Sandwell, Folding of oceanic lithospheric, *J. Geophys. Res., 90*, 8563–8569, 1985.

Mouginis-Mark, P. J., V. L. Sharpton, and B. R. Hawke, Schiaparelli Basin, Mars: Morphology tectonics and infilling history, *Proc. Lunar Planet. Sci. Conf., 12th*, 155–172, 1981.

Peeples, W. J., R. W. Sill, T. W. May, S. H. Ward, R. J. Phillips, R. L. Jordan, E. A. Abott, and T. J. Killpack, Orbital radar evidence for lunar subsurface layering in Maria Serenitatis and Crisium, *J. Geophys. Res., 83*, 3459–3468, 1978.

Pfaff, V. J., and A. M. Johnson, Opposite senses of fold asymmetry, *Eng. Geol., 27*, 3–38, 1989.

Plescia, J. B., and M. P. Golombek, Origin of planetary wrinkle ridges based on the study of terrestrial analogs, *Geol. Soc. Am. Bull., 97*, 1289–1299, 1986.

Plescia, J. B., and R. S. Saunders, Tectonics of the Tharsis region, Mars, *J. Geophys. Res., 87*, 9775–9791, 1982.

Price, E. H., Structural geometry, strain distribution, and tectonic evolution of Umtanum Ridge at Priest Rapids, and a comparison with other selected localities within Yakima fold structures, south-central Washington, Ph.D. dissertation, Wash. State Univ., Pullman, 1982.

Raitala, J. T., Highland wrinkle ridges on Mars (abstract), *Lunar Planet. Sci. XVIII*, 814–815, 1987.

Raitala, J. T., Superposed ridges on the Hesperia Planum area on Mars, *Earth, Moon Planets, 40*, 71–99, 1988.

Reidel, S. P., The Saddle Mountains: The evolution of an anticline in the Yakima fold belt, *Am. J. Sci., 284*, 942–978, 1984.

Reidel, S. P., T. L. Tolan, P. R. Hooper, K. R. Fecht, M. H. Beeson, R. D. Bentley, and J. L. Anderson, The Grande Ronde Basalt, Columbia River Basalt Group: Stratigraphic descriptions and correlations in Washington, Oregon, and Idaho, in Volcanism and Tectonism in the Columbia River Flood-Basalt Province, edited by S. P. Reidel and P. R. Hooper, *Spec. Pap. Geol. Soc. Am., 238*, 21–53, 1989*a*.

Reidel, S. P., K. R. Fecht, M. C. Hagood, and T. L. Tolan, The geologic evolution of the central Columbia Plateau, in Volcanism and Tectonism in the Columbia River Flood-Basalt Province, edited by S. P. Reidel and P. R. Hooper, *Spec. Pap. Geol. Soc. Am., 238*, 247–264, 1989*b*.

Robinson, M. S., and K. L. Tanka, Stratigraphy of the Kasei Valles region, Mars (abstract), in MEVTV Workshop on Nature and Composition of Surface Units on Mars, edited by J. R. Zimbelman, S. C. Solomon, and V. L. Sharpton, pp. 106–108, LPI Tech Rep. 88-05, Lunar and Planet. Inst., Houston, Tex., 1988.

Rubey, W. W., and M. K. Hubbert, Overthrust belt in geosynclinal area of western Wyoming in light of fluid-pressure hypothesis, *Geol. Soc. Am. Bull., 70*, 167–205, 1959.

Saunders, R. S., and T. E. Gregory, Tectonic implications of Martian ridged plains (abstract), in Reports of Planetary Geology Program, 1980, *NASA Tech. Memo., TM82385*, 93–94, 1980.

Saunders, R. S., T. G. Bills, and L. Johansen, The ridged plains of Mars (abstract), *Lunar Planet. Sci., XII*, 924–925, 1981.

Scott, D. H., and K. L. Tanaka, Geologic map of the western equatorial region of Mars, *Map I-1802-A*, U.S. Geol. Surv., Denver, Colo., 1986.

Sleep, N. H., and R. J. Phillips, Gravity and lithospheric stress on

the terrestrial planets with reference to the Tharsis region of Mars, *J. Geophys. Res.*, *90*, 4469–4489, 1985.

Solomon, S. C., and J. W. Head, Evolution of the Tharsis province of Mars: The importance of heterogeneous lithospheric thickness and volcanic construction, *J. Geophys. Res.*, *87*, 9755–9774, 1982.

Squyres, S. W., Urey prize lecture: Water on Mars, *Icarus*, *79*, 229–288, 1989.

Squyres, S. W., and M. H. Carr, Geomorphic evidence for the distribution of ground ice on Mars, *Science*, *231*, 249–252, 1986.

Strom, R. G., Lunar mare ridges, rings and volcanic ring complexes, *Mod. Geol.*, *2*, 133–157, 1972.

Talwani, P., Nur, A., and R. L. Kovach, Compressional and shear wave velocities in granular materials to 2.5 kilobars, *J. Geophys. Res.*, *78*, 6899–6909, 1973.

Tolan, T. L., S. P. Reidel, M. H. Beeson, J. L. Anderson, K. R. Fecht, and D. A. Swanson, Revisions to the estimates of the areal extent and volume of the Columbia River Basalt Group, in Volcanism and Tectonism in the Columbia River Flood-Basalt Province, edited by S. P. Reidel and P. R. Hooper, *Spec. Pap. Geol. Soc. Am.*, *238*, 1–20, 1989.

Turcotte, D. L., and G. Schubert, *Geodynamics: Application of Continuum Physics to Geological Problems*, 450 pp., John Wiley, New York, 1982.

Vink, G. E., W. J. Morgan, and W. L. Zhao, Preferential rifting of continents: A source of displaced terrains, *J. Geophys. Res.*, *89*, 10,072–10,076, 1984.

Wahrhaftig, C., and A. Cox, Rock glaciers in the Alaska Range, *Geol. Soc. Am. Bull.*, *70*, 383–436, 1959.

Watkins, J. S., and R. L. Kovack, Seismic investigation of the lunar regolith, *Proc. Lunar Sci. Conf.*, *4th*, 2561–2547, 1973.

Watters, T. R., Thin and thick-skinned deformation in the Tharsis region of Mars (abstract), in Reports of Planetary Geology Program, 1986, *NASA Tech. Memo.*, *TM89810*, 481–483, 1987.

Watters, T. R., Wrinkle ridge assemblages on the terrestrial planets, *J. Geophys. Res.*, *93*, 10,236–10,254, 1988*a*.

Watters, T. R., Periodically spaced wrinkle ridges in ridged plains units on Mars (abstract), in MEVTV Workshop on Tectonic and Volcanic Evolution of Mars, edited by H. Frey, *LPI Tech Rep. 89-04*, pp. 85–87, Lunar and Planet. Inst., Houston, Tex., 1988*b*.

Watters, T. R., Periodically spaced anticlines of the Columbia Plateau, in Volcanism and Tectonism in the Columbia River Flood-Basalt Province, edited by S. P. Reidel and P. R. Hooper, *Spec. Pap. Geol. Soc. Am.*, *238*, 283–292, 1989*a*.

Watters, T. R., Periodically spaced wrinkle ridges on the Tharsis Plateau of Mars, in *Fourth International Conference on Mars, Program and Abstracts*, pp. 206–207, NASA, Tucson, Ariz., 1989*b*.

Watters, T. R., and D. J. Chadwick, Crosscutting periodically spaced first-order ridges in the ridged plains of Hesperia Planum: Another case for a buckling model (abstract), in *MEVTV Workshop on Tectonic Features on Mars*, edited by T. R. Watters and M. P. Golombek, pp. 36–38, Lunar and Planetary Institute, Houston, Tex., 1989.

Watters, T. R., and T. A. Maxwell, Crosscutting relations and relative ages of ridges and faults in the Tharsis region of Mars, *Icarus*, *56*, 278–298, 1983.

Watters, T. R., and T. A. Maxwell, Mechanisms of basalt-plains ridge formation (abstracts), in Reports of Planetary Geology Program, 1984, *NASA Tech. Memo.*, *TM-87563*, 479–481, 1985*a*.

Watters, T. R., and T. A. Maxwell, Fold model for ridges of the Tharsis region of Mars (abstract), *Lunar Planet. Sci.*, *XVI*, 897–898, 1985*b*.

Watters, T. R., and T. A. Maxwell, Orientation, relative age, and extent of the Tharsis Plateau ridge system, *J. Geophys. Res.*, *91*, 8113–8125, 1986.

Wilhelms, D. E., and R. J. Baldwin, The role of igneous sills in shaping the Martian uplands, *Proc. Lunar Planet. Sci. Conf.*, *19th*, 355–365, 1989.

Willemann, R. J., and D. L. Turcotte, The role of lithospheric stress in the support of the Tharsis rise, *J. Geophys. Res.*, *87*, 9793–9801, 1982.

Woronow, A., Variation in the thickness of ejecta cover on Mars with increasing crater density (abstract), in MEVTV Workshop on Nature and Composition of Surface Units on Mars, edited by J. R. Zimbelman, S. C. Solomon, and V. L. Sharpton, *LPI Tech Rep. 88-05*, pp. 135–137, Lunar and Planet. Inst., Houston, Tex., 1988.

Zuber, M. T., Compression of oceanic lithosphere: An analysis of intraplate deformation in the Central Indian Basin, *J. Geophys. Res.*, *92*, 4817–4825, 1987.

Zuber, M. T., and L. L. Aist, The shallow structure of the lithosphere in the Coprates and Lunae Planum regions of Mars from geometries of volcanic plains ridges (abstract), in *MEVTV Workshop: Early Tectonic and Volcanic Evolution of Mars*, pp. 75–77, Lunar and Planetary Institute, Houston, Tex., 1988.

Zuber, M. T., and L. L. Aist, Lithospheric control in the development of the Martian plains ridges (abstract), *Lunar Planet. Sci.*, *XX*, 1261–1262, 1989.

Zuber, M. T., and L. L. Aist, The shallow structure of the Martian lithosphere in the vicinity of the ridged plains, *J. Geophys. Res.*, *95*, 14,215–14,230, 1990.

T. R. Watters, Center for Earth and Planetary Studies, National Air and Space Museum, Smithsonian Institution, Washington, DC 20560.

(Received January 17, 1989;
revised April 22, 1991;
accepted May 24, 1991.)